Inorg. Chem. **2004**, *43*, 3492–3499

Diimine–Acetylide Compounds of Ruthenium: The Structural and Spectroscopic Effects of Oxidation

Christopher J. Adams*,† and Simon J. A. Pope‡

School of Chemistry, University of Bristol, Bristol BS8 1TS, U.K., and Department of Chemistry, The University of Manchester, Manchester M13 9PL, U.K.

Received October 13, 2003

The reaction of $Ru(Me_2bipy)(PPh_3)_2Cl_2$ **1** with terminal alkynes HCCR in the presence of $TlPF_6$ leads to the formation of the vinylidene compounds $[Ru(Me_2bipy)(PPh_3)_2Cl(=C=CHR)][PF_6]$ (**2**) (**2a**, R = Bu^t; **2b**, R = *p*-C_6H_4–Me; **2c**, R = Ph). These compounds decompose in oxygenated solution to form the carbonyl compound $[Ru(Me_2bipy)(PPh_3)_2Cl(CO)][PF_6]$ (**3**), and may be deprotonated by K_2CO_3 to give the ruthenium(II) terminal acetylide compounds $Ru(Me_2bipy)(PPh_3)_2Cl(C\equiv C–R)$ (**4**) (**4a**, R = Bu^t; **4b**, R = *p*-C_6H_4–Me; **4c**, R = Ph). Cyclic voltammetry shows that **2a**–**c** may also be reductively dehydrogenated to form **4a**–**c**. **4a**–**c** are readily oxidized to their ruthenium(III) analogues $[\mathbf{4a}]^+$–$[\mathbf{4c}]^+$, and the changes seen in their UV/visible spectra upon performing this oxidation are analyzed. These show that whereas the UV/visible spectra of **4a**–**c** show MLCT bands from the ruthenium atom to the bipyridyl ligand, those of $[\mathbf{4a}]^+$–$[\mathbf{4c}]^+$ contain LMCT bands originating on the acetylide ligands. This is in agreement with the IR and ESR spectra of $[\mathbf{4a}]^+$–$[\mathbf{4c}]^+$. The X-ray crystal structures of the redox pair **4a** and $[\mathbf{4a}][\mathbf{PF_6}]$ have been determined, allowing the bonding within the metal–acetylide unit to be analyzed, and an attempt is made to determine Lever electrochemical parameters (E_L) for the vinylidene and acetylide ligands seen herein. Room temperature luminescence measurements on **4a**–**c** show that the compounds are not strongly emissive.

Introduction

There have been several recent reports on the synthesis and chemistry of compounds of the general formula bipyridyl−platinum−bis(acetylide).[1−11] These compounds have been shown to possess a metal-based HOMO and a LUMO based upon a π^* orbital on the bipyridyl, and have metal-to-ligand charge-transfer bands in the visible region of the electromagnetic spectrum. Furthermore, the compounds photoluminesce from a ^{3}MLCT state in both fluid and frozen solution.

The same trans arrangement of bipyridyl and acetylide ligands may be envisaged about the equatorial plane of an octahedral ruthenium complex. Ruthenium−bipyridyl systems are well-known luminophores, so this property of the platinum systems may be preserved upon changing the metal, but potentially there are several additional properties that might ensue. For example, the susceptibility of ruthenium(II) compounds to oxidation may allow some kind of electrochemical switching of optical properties, and the need to occupy the axial positions at the metal with ancillary ligands offers both a route into enhanced solubility and, by varying these ligands, the opportunity to "tune" the electronic properties of the compounds. No ruthenium compounds containing both a bipyridine and two acetylide ligands have been reported before; in reporting details of the chemistry of bipyridyl−ruthenium−mono(acetylide) systems, with the axial positions of the central ruthenium atom occupied by two triphenylphosphine ligands, this work contains details

* Author to whom correspondence should be addressed. E-mail: chcja@bris.ac.uk.
† University of Bristol.
‡ The University of Manchester.

(1) Adams, C. J.; James, S. L.; Liu, X.; Raithby, P. R.; Yellowlees, L. J. *J. Chem. Soc., Dalton Trans.* **2000**, 63−67.
(2) Hissler, M.; Connick, W. B.; Geiger, D. K.; McGarrah, J. E.; Lipa, D.; Lachicotte, R. J.; Eisenberg, R. *Inorg. Chem.* **2000**, *39*, 447−457.
(3) Whittle, C. E.; Weinstein, J. A.; George, M. W.; Schanze, K. S. *Inorg. Chem.* **2001**, *40*, 4053−4062.
(4) McGarrah, J. E.; Kim, Y.-J.; Hissler, M.; Eisenberg, R. *Inorg. Chem.* **2001**, *40*, 4510−4511.
(5) Chan, S.-C.; Chan, M. C. W.; Wang, Y.; Che, C.-M.; Cheung, K.-K.; Zhu, N. *Chem. Eur. J.* **2001**, 4180−4190.
(6) Wadas, T. J.; Lachicotte, R. J.; Eisenberg, R. *Inorg. Chem.* **2003**, *42*, 3772−3778.
(7) McGarrah, J. E.; Eisenberg, R. *Inorg. Chem.* **2003**, *42*, 4355−4365.
(8) James, S. L.; Younus, M.; Raithby, P. R.; Lewis, J. *J. Organomet. Chem.* **1997**, *543*, 233−235.
(9) Pomestchenko, I. E.; Luman, C. R.; Hissler, M.; Ziessel, R.; Castellano, F. N. *Inorg. Chem.* **2003**, *42*, 1394−1396.
(10) Kang, Y.; Lee, J.; Song, D.; Wang, S. *J. Chem. Soc., Dalton Trans.* **2003**, 3493−3499.
(11) Lu, W.; Chan, M. C. W.; Zhu, N.; Che, C.-M.; He, Z.; Wong, K.-Y. *Chem. Eur. J.* **2003**, 6155−6166.

10.1021/ic035181v CCC: $27.50
Published on Web 04/24/2004

of studies toward the synthesis of such compounds. The only reported compound containing both an acetylide ligand and bipyridine coordinated to a ruthenium atom is [Ru(bipy)-$(PPh_3)_2$(CO)(−C≡C−$(CH_2)_2CH_2Cl$)][PF_6].[12]

The aforementioned platinum systems are synthesized by a copper(I) iodide catalyzed Sonogashira coupling of the bipyridyl−metal−dichloride with a terminal alkyne in the presence of a base. This procedure works for a wide variety of platinum systems, but is less commonly used for ruthenium systems because of the instability of many ruthenium compounds to the strong base required. A common alternative involves the reaction of a coordinatively unsaturated 16-electron ruthenium fragment with a terminal alkyne to generate a vinylidene compound (via η^2 coordination of the alkyne followed by a 1,2-hydrogen migration), followed by deprotonation with a mild base to give the desired acetylide product.[13] This is the method employed herein.

Experimental Section

All new compounds are air stable in the solid state and reasonably air stable in solution, but standard inert-atmosphere techniques were used throughout. All solvents were purified using an Anhydrous Engineering Grubbs-type solvent system.[14] The starting material Ru(Me_2bipy)(PPh_3)$_2Cl_2$ (**1**) was prepared by literature methods,[15] and all other chemicals were used as purchased. IR and UV/visible spectra were recorded in dichloromethane solution on a Perkin-Elmer 1600 series FTIR spectrometer and a Perkin-Elmer λ-19 spectrophotometer, respectively. Cyclic voltammetry was carried out under an atmosphere of nitrogen using the standard three electrode configuration, with platinum working and counter electrodes, an SCE reference electrode, dichloromethane as solvent, 0.1 M [Bu_4N][PF_6] as electrolyte and $FeCp_2$ or $FeCp^*_2$ as internal calibrant, and a substrate concentration of approximately 1 mM. All potentials are reported vs the SCE reference electrode, against which the $FeCp_2$/[$FeCp_2$]$^+$ couple comes at 0.46 V and $FeCp^*_2$/[$FeCp^*_2$]$^+$ is −0.02 V.[16] The anisotropic ESR spectra of [**4a**]$^+$−[**4c**]$^+$ were recorded on a Bruker ESP300E X-band spectrometer calibrated with dpph in frozen 2:1 thf CH_2Cl_2 solution. NMR spectra were recorded in CD_2Cl_2 on a JEOL ECP300 spectrometer, at 300 MHz (^{1}H) and 121 MHz (^{31}P), and referenced to external TMS and external 85% H_3PO_4, respectively. UV/visible spectroelectrochemical measurements were performed in CH_2Cl_2 at 243 K using a locally constructed OTTLE (optically transparent thin-layer electrode) cell in a Perkin-Elmer λ-19 spectrophotometer, as described previously.[17] Luminescence measurements were conducted using a Perkin-Elmer LS55 fluorimeter. Microanalyses were carried out by the staff of the Microanalytical Service of the School of Chemistry at the University of Bristol.

Syntheses. [Ru(Me_2bipy)(PPh_3)$_2$Cl(=C=CHBu^t)][PF_6]·0.5Et_2O (2a·0.5Et_2O). 1 (0.191 g, 0.216 mmol), 0.075 g of TlPF_6 (0.216 mmol), and 0.2 cm^3 (1.62 mmol) of *tert*-butylacetylene were stirred in 10 cm^3 of CH_2Cl_2 for 2 h. The resulting yellow-brown solution was then filtered through a filter-paper-tipped cannula to remove the white precipitate of TlCl, and 25 cm^3 of diethyl ether was added. Upon refrigeration, orange crystals of [Ru(Me_2bipy)(PPh_3)$_2$Cl(=C=CH^{t}Bu)][PF_6]·$^1/_2C_4H_{10}O$ were formed, which were isolated by filtration, washed with diethyl ether, and dried under vacuum to give 0.213 g (0.191 mmol, 88%) of product. ^{1}H NMR (CD_2Cl_2) δ: 0.95 (9H, s, ^{t}Bu); 2.35, 2.38 (each 3H, s, Me); 3.28 (1H, t, $^4J_{HP}$ = 3.3 Hz, $H_{vinylidene}$); 6.24 (1H, d, $^3J_{HH}$ = 6.1 Hz, H_{bipy}); 6.58 (1H, d, $^3J_{HH}$ = 5.8 Hz, H_{bipy}); 7.03−7.27 (31H, m, H_{bipy} and H_{Ph}); 7.85, 7.90 (each 1H, s, H_{bipy}); 8.34 (1H, d, $^3J_{HH}$ = 5.8 Hz, H_{bipy}). ^{31}P NMR (CD_2Cl_2) δ: 20.8 (s). FAB$^+$: *m*/*z* 927 [M]$^+$. Anal. Calcd for $C_{56}H_{57}N_2RuP_3F_6ClO_{0.5}$: C, 60.62; H, 5.18; N, 2.52. Found: C, 60.67; H, 4.87; N, 2.73.

[Ru(Me_2bipy)(PPh_3)$_2$Cl(=C=CH-*p*-C_6H_4−Me)][PF_6] (2b). 1 (0.287 g, 0.33 mmol), 0.114 g (0.33 mmol) of TlPF_6, and 0.1 cm^3 (0.79 mmol) of 4-ethynyltoluene were stirred for 2 h in 30 cm^3 of CH_2Cl_2. The resulting orange-brown suspension was filtered through a filter-paper-tipped cannula to remove precipitated TlCl, and 50 cm^3 of diethyl ether was added to the stirred filtrate. On refrigeration, yellow-brown crystals of the desired product were formed, which were isolated by filtration, washed with diethyl ether, and dried under vacuum. Yield: 0.218 g (0.20 mmol, 61%). ^{1}H NMR (CD_2Cl_2) δ: 2.29, 2.37, 2.38 (each 3H, s, Me); 4.70 (1H, t, $^4J_{HP}$ = 3.5 Hz, $H_{vinylidene}$); 6.16 (1H, d, $^3J_{HH}$ = 5 Hz, H_{bipy}); 6.64 (1H, d, $^3J_{HH}$ = 5.8 Hz, H_{bipy}); 6.83 (2H, d, $^3J_{HH}$ = 8 Hz, Tol); 6.92 (1H, d, $^3J_{HH}$ = 5 Hz, H_{tolyl}); 6.97−7.24 (32H, m, H_{bipy} and H_{Ph}); 7.93 (2H, s, H_{bipy}); 8.34 (1H, d, $^3J_{HH}$ = 5.8 Hz, H_{bipy}). ^{31}P NMR (CD_2Cl_2) δ: 21.0 (s). FAB$^+$: *m*/*z* 962 [M + H]$^+$. Anal. Calcd for $C_{57}H_{50}N_2RuP_3F_6Cl$: C, 61.87; H, 4.55; N, 2.53. Found: C, 61.35; H, 4.58; N, 2.56.

[Ru(Me_2bipy)(PPh_3)$_2$Cl(=C=CHC_6H_5)][PF_6] (2c). 1 (0.325 g, 0.37 mmol), 0.129 g of TlPF_6 (0.37 mmol), and 0.1 cm^3 of phenylacetylene (1.05 mmol) were stirred for 2 h in 30 cm^3 of CH_2Cl_2 to give a cloudy solution. This was filtered, and 60 cm^3 of diethyl ether was added. Upon refrigeration, the solution deposited orange-brown crystals of **2c**, which were isolated by filtration, washed with diethyl ether, and dried in vacuo. Yield: 0.288 g (0.26 mmol, 70%). ^{1}H NMR (CD_2Cl_2) δ: 2.37, 2.39 (each 3H, s, Me); 4.75 (1H, t, $^4J_{HP}$ = 3.5 Hz, $H_{vinylidene}$); 6.19 (1H, d, $^3J_{HH}$ = 5.8 Hz, H_{bipy}); 6.64 (1H, d, $^3J_{HH}$ = 5.8 Hz, H_{bipy}); 6.92−7.25 (36H, m, H_{bipy} and H_{Ph}); 7.95 (2H, s, H_{bipy}); 8.33 (1H, d, $^3J_{HH}$ = 5.8 Hz, H_{bipy}). ^{31}P NMR (CD_2Cl_2) δ: 20.7 (s). FAB$^+$: *m*/*z* 947 [M]$^+$. Anal. Calcd for $C_{56}H_{48}N_2RuP_3F_6Cl$: C, 61.57; H, 4.43; N, 2.56. Found: C, 61.76; H, 4.63; N, 2.38.

[Ru(Me_2bipy)(PPh_3)$_2$Cl(CO)][PF_6] (3). 1 (0.151 g, 0.17 mmol) and 0.060 g of TlPF_6 (0.17 mmol) were stirred in 10 cm^3 of CH_2Cl_2 for 1 h under a carbon monoxide atmosphere. The resulting bright yellow suspension was then filtered through a filter-paper-tipped cannula to remove the white precipitate of TlCl, and 15 cm^3 of diethyl ether was added. Upon standing, pale yellow crystals of **3** were formed, which were isolated by filtration, washed with diethyl ether, and dried under vacuum to give 0.136 g (0.13 mmol, 77%) of product, which may be recrystallized as yellow-green plates by allowing vapor diffusion of diethyl ether into a dichloromethane solution. ^{1}H NMR (CD_2Cl_2) δ: 2.35, 2.47 (each 3H, s, Me); 6.22 (1H, d, $^3J_{HH}$ = 5.8 Hz, H_{bipy}); 6.68 (1H, d, $^3J_{HH}$ = 5.8 Hz, H_{bipy}); 7.15−7.35 (31H, m, H_{bipy} and H_{Ph}); 7.90, 8.04 (each 1H, s, H_{bipy}); 8.28 (1H, d, $^3J_{HH}$ = 5.8 Hz, H_{bipy}). ^{31}P NMR (CD_2Cl_2) δ: 27.1 (s). FAB$^+$: *m*/*z* 873 [M]$^+$. FT-IR (CH_2Cl_2) ν(C≡O) (cm^{-1}): 1964. Anal. Calcd for $C_{49}H_{42}N_2RuOP_3F_6Cl$: C, 57.80; H, 4.16; N, 2.75. Found: C, 57.74; H, 4.00; N, 2.74.

[Ru(Me_2bipy)(PPh_3)$_2$Cl(−C≡C−Bu^t)] (4a). 2a·0.5Et_2O (0.096 g, 0.086 mmol) and 0.050 g of potassium carbonate (0.36 mmol)

(12) Santos, A.; Lopez, J.; Galan, A.; Gonzalez, J. J.; Tinoco, P.; Echavarren, A. M. *Organometallics* **1997**, *16*, 3482−3488.
(13) Long, N. J.; Williams, C. K. *Angew. Chem., Int. Ed.* **2003**, *42*, 2586−2617.
(14) Pangborn, A. B.; Giardello, M. A.; Grubbs, R. H.; Rosen, R. K.; Timmers, F. J. *Organometallics* **1996**, *15*, 1518−1520.
(15) Adams, C. J. *J. Chem. Soc., Dalton Trans.* **2002**, 1545−1550.
(16) Connelly, N. G.; Geiger, W. E. *Chem. Rev.* **1996**, *96*, 877−910.
(17) Lee, S.-M.; Kowallick, R.; Marcaccio, M.; McCleverty, J. A.; Ward, M. D. *J. Chem. Soc., Dalton Trans.* **1998**, 3443−3450.

were stirred overnight in 10 cm^3 of thf; 10 cm^3 of hexane was added to the resulting solution, which was then filtered and evaporated to dryness. The brown solid thus obtained was redissolved in 10 cm^3 of toluene, and then 10 cm^3 of hexane was added to the resulting solution, which was filtered. Storage at 4 °C for 72 h gave the desired product as a brown microcrystalline solid, which was isolated by filtration, washed with hexane, and dried under vacuum to yield 0.040 g (0.043 mmol, 50%) of **4a**. Large cubic crystals of **4a**·$C_4H_{10}O$ for X-ray structure determination were isolated from a dichloromethane/diethyl ether solution of the compound stored at −10 °C. ^{1}H NMR (CD_2Cl_2 + [NEt_4]Cl) δ: 1.03 (9H, s, ^{t}Bu), 2.10, 2.20 (each 3H, s, Me), 5.85 (1H, d, $^3J_{HH}$ = 6.0 Hz, H_{bipy}), 6.46 (1H, d, $^3J_{HH}$ = 5.8 Hz, H_{bipy}), 6.93−7.08 (18H, m, H_{Ph}), 7.30, 7.39 (each 1H, s, H_{bipy}), 7.52−7.60 (12H, m, H_{Ph}), 8.34 (1H, d, $^3J_{HH}$ = 6.0 Hz, H_{bipy}), 8.61 (1H, d, $^3J_{HH}$ = 6.0 Hz, H_{bipy}). ^{31}P NMR (CD_2Cl_2 + [NEt_4]Cl) δ: 30.9 (s). FAB$^+$: *m*/*z* 926 [M]$^+$. FT-IR (CH_2Cl_2) ν(C≡C) (cm^{-1}): 2078. Anal. Calcd for $C_{54}H_{51}N_2RuP_2Cl$: C, 70.01; H, 5.55; N, 3.02. Found: C, 70.41; H, 5.84; N, 2.89.

[Ru(Me$_2$bipy)(PPh$_3$)$_2$Cl(−C≡C-*p*-C$_6$H$_4$−CH$_3$)] (4b). 2b (0.092 g, 0.083 mmol) and 0.092 g of potassium carbonate (0.66 mmol) were stirred overnight in 10 cm^3 of CH_2Cl_2; 20 cm^3 of hexane was added to the resulting brown solution, which was then filtered and evaporated to dryness in vacuo. The brown solid thus obtained was extracted in 10 cm^3 of toluene, and this solution was filtered and reduced in volume under vacuum until some solid material began to appear. Storage at 4 °C overnight gave the product as brown crystals, which were isolated by filtration, washed with hexane, and dried under vacuum to give 0.052 g (0.054 mmol, 65%) of **4b**. ^{1}H NMR (CD_2Cl_2 + [NEt_4]Cl) δ: 2.11, 2.18, 2.23 (each 3H, s, Me), 5.87 (1H, d, $^3J_{HH}$ = 6.2 Hz, H_{bipy}), 6.55 (1H, d, $^3J_{HH}$ = 5.8 Hz, H_{bipy}), 6.76−6.82 (4H, m, C_6H_4), 6.90−7.08 (18H, m, H_{Ph}), 7.34, 7.45 (each 1H, s, H_{bipy}), 7.48−7.57 (12H, m, H_{Ph}), 8.15 (1H, d, $^3J_{HH}$ = 6.0 Hz, H_{bipy}), 8.71 (1H, d, $^3J_{HH}$ = 5.8 Hz, H_{bipy}). ^{31}P NMR (CD_2Cl_2 + [NEt_4]Cl) δ: 31.1 (s). FAB$^+$: *m*/*z* 960 [M]$^+$. FT-IR (CH_2Cl_2) ν(C≡C) (cm^{-1}): 2067, 2043sh. Anal. Calcd for $C_{57}H_{49}N_2RuP_2Cl$: C, 71.28; H, 5.14; N, 2.92. Found: C, 71.40; H, 5.10; N, 2.53.

[Ru(Me$_2$bipy)(PPh$_3$)$_2$Cl(−C≡C−C$_6$H$_5$)] (4c). 2c (0.098 g, 0.089 mmol) and 0.098 g of potassium carbonate (0.70 mmol) were stirred overnight in 10 cm^3 of CH_2Cl_2; 20 cm^3 of hexane was added to the resulting solution, which was then filtered and evaporated to dryness in vacuo. The brown solid thus obtained was extracted in 10 cm^3 of toluene, and this solution was filtered and reduced in volume under vacuum until about to crystallize. Storage at 4 °C for 3 days gave the product as brown crystals, which were isolated by filtration, washed with hexane, and dried under vacuum to give 0.043 g (0.045 mmol, 51%) of **4c**. ^{1}H NMR (CD_2Cl_2 + [NEt_4]Cl) δ: 2.11, 2.22 (each 3H, s, Me), 5.88 (1H, d, $^3J_{HH}$ = 6.0 Hz, H_{bipy}), 6.55 (1H, d, $^3J_{HH}$ = 5.8 Hz, H_{bipy}), 6.82−7.08 (23H, m, H_{Ph}), 7.31, 7.43 (each 1H, s, H_{bipy}), 7.48−7.56 (12H, m, H_{Ph}), 8.15 (1H, d, $^3J_{HH}$ = 6.0 Hz, H_{bipy}), 8.72 (1H, d, $^3J_{HH}$ = 5.8 Hz, H_{bipy}). ^{31}P NMR (CD_2Cl_2 + [NEt_4]Cl) δ: 31.2 (s). FAB$^+$: *m*/*z* 684 [M − PPh_3]$^+$. FT-IR (CH_2Cl_2) ν(C≡C) (cm^{-1}): 2063. Anal. Calcd for $C_{56}H_{47}N_2RuP_2Cl$: C, 71.07; H, 5.01; N, 2.96. Found: C, 71.42; H, 4.94; N, 3.40.

[Ru(Me$_2$bipy)(PPh$_3$)$_2$Cl(−C≡C−Bu^t)][PF$_6$]·2.5thf ([4a][PF$_6$]·2.5thf). 4a (0.028 g, 0.03 mmol) and 0.010 g (0.03 mmol) of ferrocenium hexafluorophosphate were dissolved in 5 cm^3 of thf to give a purple solution. To this was added 5 cm^3 of hexane, and the solution was filtered. Refrigeration for 6 h caused the formation of purple crystals of [**4a**][PF_6]·2.5thf. The supernatant liquid was removed with a syringe, and the crystals were washed with hexane

Scheme 1. Synthesis of Compounds **2a**−**c**

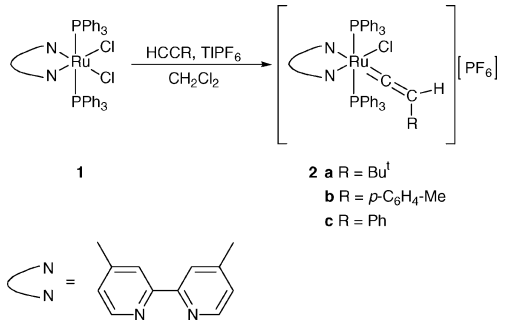

(2×5 cm^3) and dried under vacuum to give about 0.020 g (0.016 mmol, 53%) of the desired product, suitable for X-ray diffraction study. Anal. Calcd for $C_{64}H_{71}N_2RuO_{2.5}P_3ClF_6$: C, 61.41; H, 5.72; N, 2.24. Found: C, 61.96; H, 5.46; N, 2.77.

Crystal Structure Determinations. Data collection was carried out on a Bruker SMART diffractometer, with the crystal mounted in a nitrogen stream at −100 °C. Data correction was performed using the program SADABS,[18] and the structure was solved by direct methods and refined by full-matrix least-squares techniques against F^2 using the programs SHELXS-97[19] and SHELXL-97.[20] The thf molecules in the structure of [**4a**][PF_6]·2.5thf are all disordered to some extent, and were refined isotropically without the addition of hydrogen atoms.

Crystal Data. 4a·C$_4$H$_{10}$O: $C_{58}H_{61}ClN_2OP_2Ru$, M = 1000.55, orthorhombic, a = 27.180(5) Å, b = 12.912(3) Å, c = 14.454(3) Å, V = 5072.5(18) Å^3, T = 173(2) K, λ = 0.71073 Å, space group *Pna*2$_1$ (No. 33), Z = 4, μ(Mo Kα) = 0.466 mm^{-1}, 32468 reflections measured, 10671 unique (R_{int} = 0.0716), R_1 [$I > 2\sigma(I)$] = 0.0446, R_1 [all data] = 0.0866. **[4a][PF$_6$]·2.5C$_4$H$_8$O:** $C_{64}H_{51}ClF_6N_2O_{2.5}P_3Ru$, M = 1231.50, triclinic, a = 11.826(8) Å, b = 13.962(6) Å, c = 19.020(11) Å, α = 78.56(5)°, β = 87.14(4)°, γ = 80.52(6) °, V = 3035(3) Å^3, T = 173(2) K, λ = 0.71073 Å, space group $P\bar{1}$ (No. 2), Z = 2, μ(Mo Kα) = 0.444 mm^{-1}, 31738 reflections measured, 13796 unique (R_{int} = 0.0748), R_1 [$I > 2\sigma(I)$] = 0.0664, R_1 [all data] = 0.1346.

Results

Vinylidene and Carbonyl Complexes. The trans diimine−dichloride ruthenium starting material Ru(Me$_2$bipy)(PPh$_3$)$_2$Cl$_2$ **1** (Me$_2$bipy = 4,4′-dimethyl-2,2′-bipyridyl) reacts with terminal alkynes in the presence of 1 equiv of the chloride abstractor $TlPF_6$ to give the ionic vinylidene compounds [Ru(Me$_2$bipy)(PPh$_3$)$_2$Cl(=C=CHR)][PF_6] (**2a**, R = Bu^t; **2b**, R = *p*-C$_6$H$_4$−Me; **2c**, R = C_6H_5) in good yield as air stable yellow-brown solids (Scheme 1). Analytical and spectroscopic data are in accordance with their formulation and are comparable with those reported in the literature for other ruthenium−vinylidene compounds; thus their ^{1}H NMR spectra contain a characteristic signal at between 3 and 5 ppm for the vinylidene proton. The trans nature of the triphenylphosphine ligands is confirmed by the splitting of this vinylidene signal into a triplet due to coupling to two equivalent phosphorus nuclei ($^4J \approx 3.5$ Hz), and by the single

(18) Sheldrick, G. M. *SADABS*, version 2.03; University of Göttingen: Göttingen, 2001.
(19) Sheldrick, G. M. *SHELXS-97*, *Program for crystal structure solution*; University of Göttingen: Göttingen, 1997.
(20) Sheldrick, G. M. *SHELXL-97*, *Program for crystal structure refinement*; University of Göttingen: Göttingen, 1997.

Table 1. Electrochemical Data for All Compounds

	E_p/V	$E_{1/2}$/V	E_L/V
2a	−1.47	*a*	
2b	−1.35	1.11	0.47
2c	−1.39	1.19	0.55
3	−1.44	1.69	1.05
4a		0.04	−0.60
4b		0.13	−0.51
4c		0.16	−0.48

[a] No reversible oxidation process; an irreversible process with a peak potential of 1.57 V is seen.

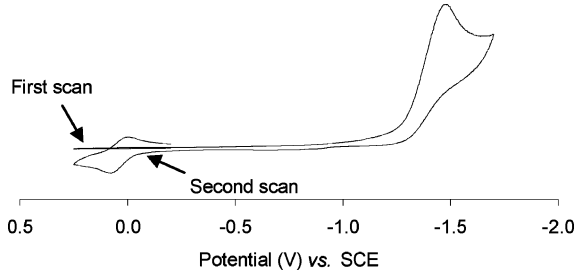

Figure 1. CV of **2a**, scanned from −0.2 V to 0.25 V to −1.7 V to 0.25 V to −0.2 V, showing how the product wave at 0.04 V is generated by the irreversible process at −1.47 V.

Scheme 2. Synthesis of Compounds **4**

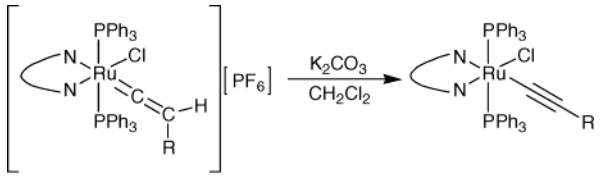

PPh_3 signal seen in the ^{31}P NMR. Compounds **2a**−**c** may also be synthesized from **1** and the appropriate alkyne with $[NH_4][PF_6]$ as the halide acceptor and anion source, but the reaction is much slower than with $TlPF_6$.

Cyclic voltammetry of **2a**−**c** shows that the compounds all display an irreversible cathodic process, at around −1.35 V (Table 1). Following this process a product wave is observed between 0 and 0.4 V, in a position corresponding to that seen in the CV of the corresponding compound **4** (vide infra) (Figure 1). Thus, reduction of the vinylidene compound generates the associated acetylide compound, presumably by the elimination of hydrogen:

$$[Ru{=}C{=}CHR]^+ + e^- \rightarrow Ru{-}C{\equiv}C{-}R + {}^1/_2H_2$$

In addition, compounds **2b** and **2c** both display a $Ru^{II/III}$ oxidation couple, at 1.11 and 1.19 V, respectively, which is almost fully reversible for **2b** and which is reversible at scan speeds above 250 mV s^{-1} for **2c**. **2a** displays only an irreversible anodic processes.

Solutions of **2a**−**c** decompose slowly in air to give the carbonyl compound $[Ru(Me_2bipy)(PPh_3)_2Cl(CO)][PF_6]$ (**3**), due to reaction between the vinylidene group and atmospheric oxygen. **3** may be deliberately synthesized by reaction of **1** with 1 equiv of $TlPF_6$ under a carbon monoxide atmosphere; it is pale yellow when pure, but is often discolored by impurities. **3** displays a reversible Ru^{II}/Ru^{III} oxidation at 1.69 V in the cyclic voltammogram, and also has an irreversible reduction at −1.44 V.

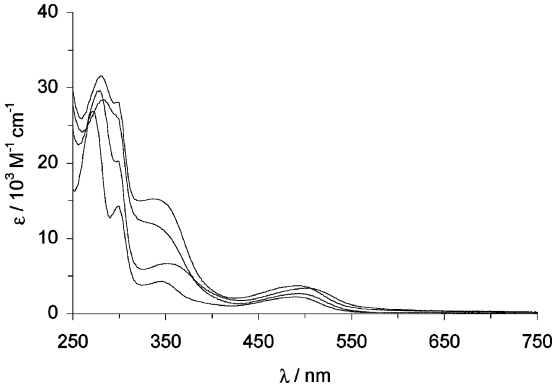

Figure 2. UV/visible spectra of **1** and **4a**−**c**. In ascending order of ϵ at 350 nm: **1**, **4a**, **4b**, **4c**.

Table 2. UV/Visible Data for **1** and **4a**−**c**

	λ_{max}/nm (ϵ/10^3 M^{-1} cm^{-1})			
1	272 (37.9)	299 (20.1)	346 (6.1)	492 (3.2)
4a	277 (29.6)	298 (20.3)	353 (6.7)	501 (3.4)
4b	283 (28.4)	299 (25.8)	331 (12.1)	493 (2.7)
4c	281 (31.6)	297 (28.0)	336 (15.3)	490 (3.7)

Acetylide Complexes. The vinylidene compounds **2a**−**c** can readily be deprotonated to form the terminal acetylide complexes $Ru(Me_2bipy)(PPh_3)_2Cl(C{\equiv}CR)$ (**4a**, R = Bu^t; **4b**, R = *p*-C_6H_4−Me; **4c**, R = C_6H_5) (Scheme 2). A number of different bases will effect this reaction, but for ease of separation a suspension of K_2CO_3 was found to be best. The solution IR spectra of the acetylide compounds each show the expected C≡C absorption between 2040 and 2080 cm^{-1}, and in addition compound **4b** displays a second C≡C feature as a shoulder at 2043 cm^{-1} on the strong absorption at 2067 cm^{-1}. The most probable explanation for this is Fermi coupling, which has been observed to create two C≡C peaks in the spectra of mono-acetylide compounds before.[21,22] This occurs when an overtone or combination band that is normally of negligible intensity is able to gain intensity through an interaction with a C≡C mode of similar energy and the same symmetry.[23] The ^{31}P NMR spectra of **4a**−**c** are broadened at room temperature, probably due to the transient loss of a chloride ion from the compounds since the spectra become sharp on the addition of $[NEt_4]Cl$ to the solution.

The UV/visible spectral data for **4a**−**c** are summarized in Table 2 and presented in Figure 2. Like the parent dichloride complex **1**, compounds **4a**−**c** have four major absorption bands in the 250−500 nm range, and in the case of **1** all but the highest energy of these have previously been attributed to ruthenium-to-bipyridyl MLCT transitions.[24] However, were this the case, then it would be expected that on oxidation of the metal center they would be shifted significantly to higher energy, or disappear altogether. This is true

(21) Denis, R.; Toupet, L.; Paul, F.; Lapinte, C. *Organometallics* **2000**, *19*, 4240−4251.
(22) Paul, F.; Mevellec, J.-Y.; Lapinte, C. *J. Chem. Soc., Dalton Trans.* **2002**, 1783−1790.
(23) Ebsworth, E. A. V.; Rankin, D. W. H.; Cradock, S. *Structural Methods in Inorganic Chemistry*; Blackwell Scientific Publications: Oxford, 1987.

Table 3. Spectroscopic Data for [**4a**]$^+$−[**4c**]$^+$

	g_x	g_y	g_z	$\langle g \rangle$	λ_{max}/nm	ν(C≡C)/cm^{-1}
[**4a**]$^+$	2.387	2.249	1.865	2.167	568	2010
[**4b**]$^+$	2.286	2.216	1.881	2.127	739, 678	1948
[**4c**]$^+$	2.370	2.281	1.860	2.170	701, 627	1959

for the two lowest energy bands (at around 490 and 330−350 nm) (vide infra), but not for the band at about 300 nm, which may therefore be assigned to a ligand localized bipy $\pi \rightarrow \pi^*$ transition. This is also the origin of the band at around 280 nm. The cyclic voltammograms of the acetylide compounds **4a**−**c** all show reversible oxidation waves corresponding to the $Ru^{II/III}$ couple at relatively low potentials, meaning that their ruthenium(III) analogues [**4a**]$^+$−[**4c**]$^+$ can be readily made by chemical or electrochemical oxidation. [**4a**][$\mathbf{PF_6}$] is stable enough to be isolated whereas salts of [**4b**]$^+$ and [**4c**]$^+$ are not, but these ions are readily generated in situ for spectroscopic characterization. Thus, ESR spectroscopy was performed on samples of **4a**−**c** oxidized by ferrocenium hexafluorophosphate under a nitrogen atmosphere in an ESR tube, and IR spectra were obtained by oxidizing solutions of **4a**−**c** with ferrocenium hexafluorophosphate and transferring the resulting solutions under nitrogen to the IR cell. Ferrocenium hexafluorophosphate is a suitable choice because both it and ferrocene are IR and ESR silent in the regions of interest, but this is not the case in the UV/visible region. Therefore, UV/visible spectra were collected spectroelectrochemically using an OTTLE cell. The integrity of the spectroelectrochemical results was checked by reversing the oxidation after the process had finished and checking that the spectrum returned to that of the starting material, and was also shown by the tight isosbestic points observed.

Spectroscopic results for the ions [**4a**]$^+$−[**4c**]$^+$ are collected in Table 3 and show that upon oxidation the energy of the C≡C absorption in the IR spectrum decreases substantially. The ESR results are similar to those reported for [**1**][$\mathbf{BF_4}$], a frozen solution giving a rhombic spectrum with closely spaced g_x and g_y values and a much lower g_z value. It should be noted that the cations [**4a**]$^+$−[**4c**]$^+$ are all air sensitive (especially [**4b**]$^+$ and [**4c**]$^+$), decomposing to **3**.

The most striking observation about the ruthenium(III) ions is their vivid color. Whereas the ruthenium(II) acetylide compounds are red-brown, the ruthenium(III) analogue [**4a**]$^+$ is magenta, and the aryl compounds [**4b**]$^+$−[**4c**]$^+$ are blue-green. This is recorded in their UV/visible spectra, whereupon oxidation of the parent ruthenium(II) compound the MLCT bands at around 490 and 330−350 nm diminishes dramatically in intensity, and a new low-energy band appears in the range 568−739 nm; as an example, the spectrum of **4c** during electrolysis is shown in Figure 3.

Crystal Structure Determinations. The structures of the redox pair of compounds **4a** and [**4a**][$\mathbf{PF_6}$] have both been determined by X-ray diffraction; that of **4a** is shown in Figure 4 and is indistinguishable to the naked eye from that of [**4a**]$^+$. A comparison of selected bond lengths and angles is given

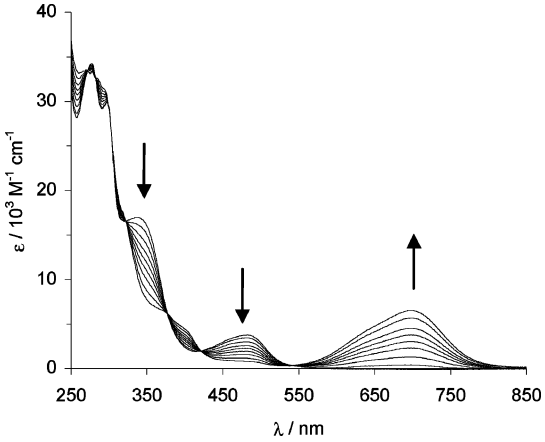

Figure 3. The UV/visible spectrum of **4c** during oxidation, showing the LMCT charge-transfer band that grows at around 700 nm.

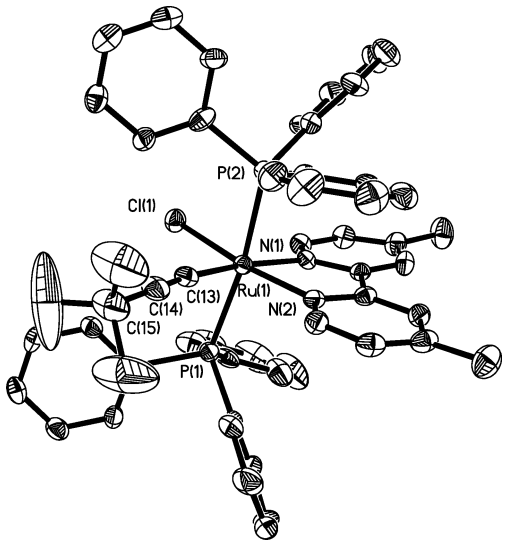

Figure 4. ORTEP plot of **4a** (ellipsoids at the 50% probability level). Hydrogen atoms have been omitted for clarity.

in Table 4 (the same numbering scheme was used in both cases), and shows that in both cases the geometry around the ruthenium atom is approximately octahedral, with deviation from this caused by the small bite angle of the bipyridyl ligand. The two axial triphenylphosphine ligands are slightly bent away from a linear trans geometry toward the space between the chloride and acetylide ligands, and the large trans influence of the acetylide ligand is shown by the ruthenium−nitrogen distances, that opposite the chloride {Ru(1)−N(2)} being shorter than that opposite the acetylide {Ru(1)−N(1)}. Otherwise the structures are unremarkable, bond lengths within the metal−acetylide fragment of the ruthenium(II) compound **4a** being similar to those reported for a number of ruthenium(II) piano-stool type complexes with the same terminal *tert*-butylacetylide ligand.[25] Variation *between* the two structures will be discussed below.

Discussion

Electrochemistry. The reductive dehydrogenation of vinylidene compounds as demonstrated for compounds **2a**−**c**

(24) Batista, A. A.; Santiago, M. O.; Donnici, C. L.; Moreira, I. S.; Healy, P. C.; Berners-Price, S. J.; Queiroz, S. L. *Polyhedron* **2001**, *20*, 2123−2128.

(25) Bruce, M. I.; Hall, B. C.; Zaitseva, N. N.; Skelton, B. W.; White, A. H. *J. Chem. Soc., Dalton Trans.* **1998**, 1793−1803.

Table 4. Selected Bond Lengths (Å) and Angles (deg) for **4a** and [**4a**]$^{+}$ [a]

bond	**4a**	[**4a**]$^{+}$	Δ	angle	**4a**	[**4a**]$^{+}$	Δ
Ru(1)−N(1)	2.120(4)	2.152(4)	+0.032(6)	P(1)−Ru(1)−P(2)	172.02(4)	174.67(5)	+2.65(6)
Ru(1)−N(2)	2.051(3)	2.091(4)	+0.040(5)	N(1)−Ru(1)−C(13)	171.17(15)	168.98(18)	−1.19(23)
Ru(1)−Cl(1)	2.4638(12)	2.3451(18)	−0.1187(22)	N(2)−Ru(1)−Cl(1)	169.16(10)	168.96(12)	−0.20(16)
Ru(1)−C(13)	2.053(5)	1.974(5)	−0.079(7)	Cl(1)−Ru(1)−C(13)	97.89(12)	98.73(16)	+0.84(20)
C(13)−C(14)	1.174(6)	1.197(7)	+0.023(9)	N(1)−Ru(1)−N(2)	78.40(14)	76.96(17)	−1.44(22)
Ru(1)−P(1)	2.3470(13)	2.385(20)	+0.0380(24)	Ru(1)−C(13)−C(14)	173.6(4)	177.2(5)	+3.6(6)
Ru(1)−P(2)	2.3697(13)	2.398(20)	+0.0283(24)	C(13)−C(14)−C(15)	176.1(6)	179.7(6)	+3.6(8)

[a] Δ is the change upon oxidation.

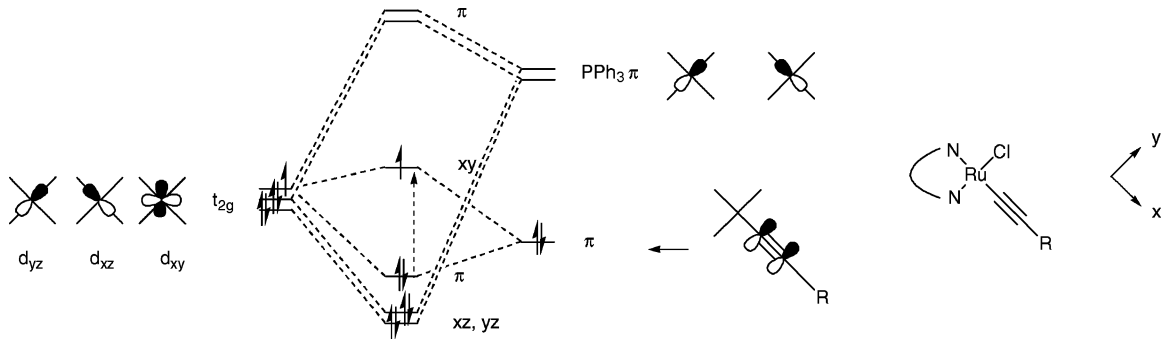

Figure 5. Qualitative MO diagram for **4a**−**c** and [**4a**]$^{+}$−[**4c**]$^{+}$, viewed down the P−Ru−P (*z*) axis, showing the interaction of the ruthenium t_{2g} orbitals with the vacant π orbitals of the triphenyphosphine and the filled π orbitals of the acetylide and chloride ligands. Interaction with the π-type orbitals of the chloride and bipyridyl ligands is not shown, but does not alter the ordering of orbitals. For the d^5 Ru(III) case (shown), the LMCT transition is shown by the dotted arrow.

is not a novel process, although it has not been seen in ruthenium compounds before; Bianchini has demonstrated that, in certain cobalt[26] and rhodium[27] systems, one-electron reduction of the vinylidene complex liberates hydrogen and forms the corresponding acetylide. Much more common is the oxidative formation of acetylide from vinylidene with accompanying loss of a proton, which has been demonstrated in a ruthenium system;[28] however, the oxidative decomposition of **2a** in the cyclic voltammogram is not accompanied by a daughter peak from the acetylide.

In recent years many ligands have been assigned E_L values, electrochemical parameters based on the additive system proposed by Lever,[29] but there does not seem to have been any attempt to do so for acetylide systems. Compounds **4a**−**c** present an opportunity to do this, especially since all the other ligands in the complex have been parametrized by Lever. Taking the published values of E_L (0.46 V for Me_2bipy, 0.39 V for PPh_3 and −0.24 V for Cl^-) predicts that $E_{1/2}$ for **1** should be 0.76 V vs NHE in acetonitrile. The published value of 0.40 V vs SCE in dichloromethane[15] allows a correction of −0.36 V to be made for differences in conditions. The difference in oxidation potential between the acetylide compounds and the dichloride compound **1** must be the same as the difference in E_L for the acetylide ligand and the chloride ligand that it replaces; so, for example, compound **4a** is oxidized at 0.04 V, 0.36 V less than **1**. Therefore, E_L for the *tert*-butylacetylide ligand must be 0.36 V less than the value for chloride (−0.24 V), equaling −0.60 V. Values derived in the same way for all the acetylide ligands in this study are shown in Table 1. The value of E_L (CO) derived in this way from the data for compound **3** is 1.05 V, which may be compared to the published value of 0.99 V to give an indication of the error involved. It is noteworthy that the published oxidation potentials (vs Ag/AgCl) of *trans*-[$RuCl_2$-$(dppe)_2$], *trans*-[RuCl(C≡CPh)$(dppe)_2$] and *trans*-[Ru-$(C≡CPh)_2(dppe)_2$] are 0.60, 0.55, and 0.56 V, respectively, which clearly indicate a nonlinear trend upon replacing chloride by phenylacetylide.[30]

A previous attempt has been made to assign E_L parameters to vinylidene ligands, though by a more indirect method.[31] The values given for tolyl− and phenyl−vinylidene were 0.51 and 0.52 V, compared to values calculated by the above method from the data for **2b** and **2c** of 0.47 and 0.55 V, respectively.

Molecular Orbitals. The ordering of the doubly occupied metal d orbitals of t_{2g} origin in **1** has been assigned as 1 over 2; that is, the d_{xz} and d_{yz} interact with the moderately π-accepting triphenylphosphine ligand and are lowered in energy, whereas the d_{xy} orbital has only in-plane π-donor interactions with the chloride and ligands, and is the HOMO.[32] This arrangement of orbitals is also true for **4a**−**c**, with the added complication of d_{xz} and d_{yz} no longer being degenerate because of the replacement of one chloride ligand with an acetylide group (Figure 5). (There has been considerable debate about the π-character of acetylide ligands over the years, but the consensus appears to be that in the

(26) Bianchini, C.; Innocenti, P.; Meli, A.; Peruzzini, M.; Zanobini, F.; Zanello, P. *Organometallics* **1990**, *9*, 2514−2522.
(27) Bianchini, C.; Meli, A.; Peruzzini, M.; Zanobini, F.; Zanello, P. *Organometallics* **1990**, *9*, 241−250.
(28) Hurst, S. K.; Cifuentes, M. P.; Morrall, J. P. L.; Lucas, N. T.; Whittall, I. R.; Humphrey, M. G.; Asselberghs, I.; Persoons, A.; Samoc, M.; Luther-Davies, B.; Willis, A. C. *Organometallics* **2001**, *20*, 4664−4675.
(29) Lever, A. B. P. *Inorg. Chem.* **1990**, *29*, 1271−1285.
(30) Powell, C. E.; Cifuentes, M. P.; Morrall, J. P.; Stranger, R.; Humphrey, M. G.; Samoc, M.; Luther-Davies, B.; Heath, G. A. *J. Am. Chem. Soc.* **2003**, *125*, 602−610.
(31) Almeida, S. S. P. R.; Pombeiro, A. J. L. *Organometallics* **1997**, *16*, 4469−4478.
(32) Chakravarty, J.; Bhattacharya, S. *Polyhedron* **1994**, *13*, 2671−2678.

majority of cases they act as π-donor ligands with little metal-to-ligand back-bonding. Replacement of chloride by acetylide should therefore cause little change in the ordering of orbitals.)[33,34] Thus, on oxidation of **4a**−**4c** from ruthenium(II) to ruthenium(III) the electron is removed from the d_{xy} orbital, creating a metal-based SOMO that causes $<g>$ to deviate from 2.00.

This MO scheme is supported by the bond lengths seen in the crystallographically determined structures of the redox pair **4a** and [**4a**][$\mathbf{PF_6}$]. Upon oxidation, the major changes in bond length are shortenings of the metal−chloride (by 0.119(2) Å) and metal−acetylide (by 0.079(7) Å) distances, consistent with the removal of an electron from a metal orbital that is antibonding with respect to both of these ligands. This must be the d_{xy} orbital, as it is the sole occupied orbital lying in the plane of both these ligands. The ruthenium−phosphorus bond lengths increase slightly (by approximately 0.04 Å), in line with previous studies on the nature of metal−phosphine bonding in redox pairs.[35]

The structures of **4a** and [**4a**][$\mathbf{PF_6}$] appear to constitute the fourth crystallographically characterized metal−acetylide redox pair; those reported previously have been [Mn(dppe)-$(C{\equiv}CPh)_2]^{0/1}$,[36] $[Fe\{P(CH_2CH_2PPh_2)_3\}(C{\equiv}CPh)]^{0/1}$,[37] and $[Mo(dppe)(\eta\text{-}C_7H_7)(C{\equiv}CPh)]^{0/1}$,[38] although the large esd's on the first two of these pairs preclude any meaningful discussion of bond length changes on oxidation. The last pair is a d^6/d^5 pair as in the current work, and shows a similar decrease (of 0.071(10) Å) in the metal−acetylide distance. These decreases provide further support for the absence of π back-bonding in metal acetylide complexes; if this interaction were present it would be bonding between the d_{xy} orbital and the ligand π system, and the metal−acetylide bond length would be expected to increase upon depopulating the resultant MO.

UV/Visible Spectra of Ru(III) Compounds. The new absorption observed in the UV/visible spectrum following oxidation of **4a**−**c** has no counterpart in the spectrum of **[1][$\mathbf{BF_4}$]**, the analogous ruthenium(III) dichloride compound, and therefore would appear to have some acetylide character. As the π orbitals of the carbon−carbon triple bond are the frontier orbitals of this ligand and the LUMO of the compound is now the metal-based d_{xy} SOMO, this band can be assigned to a $\pi \rightarrow d_{xy}$ LMCT transition. In the *tert*-butylacetylide fragment of **4a** both alkyne triple-bond π orbitals are degenerate (assuming free rotation of the *tert*-butyl group), but in the arylacetylides **4b** and **4c** they are not;[33] which of the π orbitals is the donor depends upon the (unknown) orientation of the aryl ring.

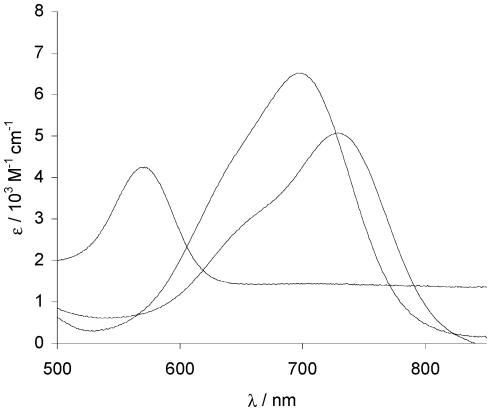

Figure 6. The LMCT bands seen in the UV/visible spectrum upon electrogeneration of $[\mathbf{4a}]^+$−$[\mathbf{4c}]^+$. In ascending order of ϵ at 650 nm: $[\mathbf{4a}]^+$, $[\mathbf{4b}]^+$, $[\mathbf{4c}]^+$.

Prior reports of the UV/visible spectra of ruthenium(III) acetylides have reported the presence of a similar LMCT band, with vibronic structure of 1730−1830 cm^{-1} in the case of $[Ru(16\text{-}TMC)(C{\equiv}CAr)_2]^+$ [39] and of 2040−2050 cm^{-1} for $[Ru(C{\equiv}CAr)_2(dppe)_2]$[30] on the high energy side of the band. The LMCT bands seen on spectroelectrochemical generation of $[\mathbf{4b}]^+$ and $[\mathbf{4c}]^+$ also contain some high energy structure, which may be fitted to Gaussian curves with maxima at the values shown in Table 3. The LMCT bands of $[\mathbf{4a}]^+$−$[\mathbf{4c}]^+$ are shown in Figure 6.

If the structure in the spectra of $[\mathbf{4b}]^+$ and $[\mathbf{4c}]^+$ is also vibronic in origin, then the vibrational spacing $\Delta\nu$ is 1223 and 1676 cm^{-1}, respectively, a wide spread of values somewhat lower than those previously reported. The values are also lower than the vibrational frequency of the triple bond involved ($[\mathbf{4b}]^+$ and $[\mathbf{4c}]^+$ have ν(C≡C) of 1948 and 1959 cm^{-1}, respectively (Table 3)), but it should be remembered that the progression relates to the spacing in the energy levels of the upper state of the transition. As the LMCT transition involves moving an electron from an orbital that is principally C≡C π-bonding in character to one that is principally metal d_{xy} (Figure 5), the vibrational frequency of the carbon−carbon bond in the excited state would be lower than in the ground state, which would be reflected in the spacing of the vibronic progression.

Luminescence Measurements

In view of the luminescent behavior of the geometrically similar platinum compounds,[2] a study of the photophysical attributes of complexes **4a**−**c** was undertaken. Measurements were conducted on dichloromethane solutions at room temperature, and excitation wavelengths were selected on the basis of absorption spectra (Table 2). For all the compounds **4a**−**c**, excitation selectively into the MLCT excited state (λ_{exc} = 340, 470 nm) resulted in no observable emission. In addition, the emissive properties of the complexes were not significantly enhanced by utilizing the aromatic chromophores; thus, in compounds **4a** and **4b** an excitation wavelength of 260 nm (intraligand π−π*) resulted

(33) Lichtenberger, D. L.; Renshaw, S. K.; Bullock, R. M. *J. Am. Chem. Soc.* **1993**, *115*, 3276−3285.
(34) McGrady, J. E.; Lovell, T.; Stranger, R.; Humphrey, M. G. *Organometallics* **1997**, *16*, 4004−4011.
(35) Orpen, A. G.; Connelly, N. G. *Organometallics* **1990**, *9*, 1206−1210.
(36) Krivykh, V. V.; Eremenko, I. L.; Veghini, D.; Petrunenko, I. A.; Pountney, D. L.; Unseld, D.; Berke, H. *J. Organomet. Chem.* **1996**, *511*, 111−114.
(37) Bianchini, C.; Laschi, F.; Masi, D.; Ottaviani, F. M.; Pastor, A.; Peruzzini, M.; Zanello, P.; Zanobini, F. *J. Am. Chem. Soc.* **1993**, *115*, 2723−2730.
(38) Beddoes, R. L.; Bitcon, C.; Whiteley, M. W. *J. Organomet. Chem.* **1991**, *402*, 85−96.
(39) Choi, M.-Y.; Chan, M. C.-W.; Zhang, S.; Cheung, K.-K.; Che, C.-M.; Wong, K.-Y. *Organometallics* **1999**, *18*, 2074−2080.

in no emission. Interestingly, under the same circumstances the phenyl derivative **4c** did show weak emission, at 463 and 526 nm.

These unremarkable emissive properties therefore indicate the presence of nonradiative decay pathways for **4a**−**c**, in contrast to related platinum(II) complexes which are brightly emissive in solution at room temperature.[2,5] It is worth noting that chloride ions are known to quench fluorescence by charge transfer from the halide to the excited state of a chromophore, and the presence of free chloride (vide supra) may be thus preventing emission from solutions of **4a**−**c**.[40]

Conclusions

The first series of ruthenium compounds with both bipyridyl and acetylide ligands has been synthesized, and it has been demonstrated that these compounds, **4a**−**c**, have redox-switchable charge-transfer transitions. However, unlike platinum−diimine−bis(acetylide) compounds and luminescent ruthenium−bipyridyl systems, compounds **4a**−**c** are not strongly emissive from fluid solution at room temperature. Current work is focused upon synthesizing bis-acetylide compounds from **4a**−**c**; as these compounds are more similar to emissive platinum species, it is hoped that they may possess stronger fluorescence.

Acknowledgment. We wish to thank the University of Bristol for a Junior Fellowship, Mr. Lifeng Zhu for the curve fitting, and Professors A. G. Orpen and M. D. Ward and Dr. S. Faulkner for helpful discussions.

Supporting Information Available: X-ray crystallographic files in CIF format for the structure determination of **4a**·Et_2O and [**4a**][PF_6]·2.5thf. This material is available free of charge via the Internet at http://pubs.acs.org.

IC035181V

(40) Goodall, W.; Williams, J. A. G. *J. Chem. Soc., Dalton Trans.* **2000**, 2893−2895.